

Primljen / Received: 10.11.2017.

Ispravljen / Corrected: 25.9.2018.

Prihvaćen / Accepted: 5.1.2019.

Dostupno online / Available online: 10.5.2019.

Seismic upgrading of isolated bridges with SF-ED devices: Analytical study validated by shaking table testing

Authors:



¹Assoc.Prof. **Misin Misini**, PhD. CE
misin.misini@uni-pr.edu



²Assist.Prof. **Jelena Ristić**, PhD. CE
jelena.ristic.ibu@gmail.com



³Prof. **Danilo Ristić**, PhD. CE
danilo.ristic@gmail.com



¹Zijadin Guri, MSc. CE
guri.zijadin@gmail.com



⁴**Nebi Pllana**, PhD. CE
nplana@ipe-proing.com

¹University of Prishtina, Faculty of Civil Engineering and Architecture, Prishtina, Kosovo

²IBU, Faculty of Engineering, Dep. of Civil Engineering, Skopje, Macedonia

³Institute of Earthquake Engineering and Engineering Seismology (IZIS), Skopje, Macedonia

⁴IPE-Proing, Prishtina, Kosovo

Original scientific paper

Misin Misini, Jelena Ristic, Danilo Ristic, Zijadin Guri, Nebi Pllana

Seismic upgrading of isolated bridges with SF-ED devices: Analytical study validated by shaking table testing

A nonlinear 3D analytical model, experimentally validated by seismic shaking table tests of a large-scale bridge model constructed with upgraded seismically isolated system with space flange devices, representing an advanced USI-SF seismic protection system, is presented. Seismic protection advances of USI-SF system are demonstrated through comparative analysis of the model prototype with the proposed new system. Technological options for qualitative upgrading of various types of isolated bridges are made possible with structural generalization of SF-ED devices.

Key words:

bridge, seismic isolation, shaking table, ductility, energy dissipation, seismic safety

Izvorni znanstveni rad

Misin Misini, Jelena Ristic, Danilo Ristic, Zijadin Guri, Nebi Pllana

Seizmičko poboljšanje mostova izoliranih uređajima SF-ED: analitičko istraživanje potvrđeno ispitivanjima na potresnom stolu

U radu je prikazan nelinearni trodimenzionalni analitički model eksperimentalno potvrđen ispitivanjima na potresnom stolu modela mosta u velikom mjerilu s poboljšanim sustavom za seizmičku izolaciju s prostornim pojasnicama, tj. s naprednim sustavom seizmičke zaštite tipa USI-SF. Prikazano je poboljšanje seizmičke zaštite pomoću sustava USI-SF usporednom analizom prototipa s predloženim novim sustavom. Tehnološke opcije za kvalitativno poboljšanje raznih tipova izoliranih mostova omogućene su konstrukcijskim poopćenjem uređaja SF-ED.

Ključne riječi:

most, seizmička izolacija, potresni stol, duktilnost, disipacija energije, seizmička sigurnost

Wissenschaftlicher Originalbeitrag

Misin Misini, Jelena Ristic, Danilo Ristic, Zijadin Guri, Nebi Pllana

Seismische Verbesserung von Brücken, die durch SF-ED Geräte isoliert sind: analytische Untersuchung bestätigt durch Untersuchungen auf dem Erdbebentisch

In der Abhandlung ist das nicht lineare dreidimensionale analytische Modell dargestellt, das experimentell durch Untersuchungen am Erdbebentisch des Brückenmodells in einem großen Maßstab mit verbessertem System der seismischen Isolierung mit räumlichen Flanschen festgestellt wurde, d. h. mit einem fortschrittlichen seismischen Typ USI-SF. Dargestellt wird die Verbesserung des seismischen Schutzes mithilfe des Systems USI-SF im Vergleich zur Analyse des Prototyps mit dem empfohlenen neuen System. Die technologischen Optionen für eine hochwertige Verbesserung unterschiedlicher Typen isolierter Brücken werden durch die strukturelle Verallgemeinerung des SF-ED Gerätes ermöglicht.

Schlüsselwörter:

Brücke, seismische Isolierung, Erdbebentisch, Duktilität, Energiedissipation, seismische Sicherheit

1. Introduction

Although the majority of the most important research in the field of seismic isolation of bridges has been performed in renowned research centres in Japan, USA, Italy, New Zealand, etc., the contributions from many other countries worldwide have recently been intensified, resulting in a large diversity of ideas and concepts. However, most frequently, theoretical or experimental research is purpose-oriented and concentrated on the development of individual devices of specific type, such as: rubber seismic bearings, sliding seismic bearings, rolling seismic bearings, displacement-limiting devices, etc. A detailed review of the concepts and achievements made in this specific field is given in comprehensive publications written by a number of authors, [1, 2]. Specific hysteretic behaviour characteristics of common rubber and lead-rubber seismic bearings are presented in [3, 4]. Specific behaviour of sliding seismic bearings [5-7], as well as of recently developed simple pendulum seismic bearings [8, 9], has been comprehensively studied, experimentally validated, [10, 11], and introduced in current practice. The application concept of the proposed additional devices for seismic energy dissipation, [12-17], along with some devices for limitation of large displacements, has been introduced. Lately, the developments in this innovative earthquake engineering field have been intensified with complementary studies of various specific related phenomena, including pounding effect [18], axial behaviour of elastomeric isolators [19], semi-active dampers [20], as well as with studies devoted to qualitative upgrading of present technologies. Seismic design regulations of seismically isolated bridges are gradually being introduced, and are permanently upgraded [21], and implemented in many countries located in seismically active regions [22]. In research conclusions, most of the authors give recommendations about the need for conducting further studies in this scientific field and, also, for creating new ideas aimed at upgrading the existing bridge isolation systems. The intolerable damage and total collapse of bridge systems, as observed during recent strong earthquakes, have become a very strong argument to widely start rapid development and practical implementation of various seismic isolation systems for the seismic protection of bridges. The present development research has been planned and conducted in response to the potential future risk and catastrophic impacts on classical and common isolated bridges under strong earthquake action. The research resulted in the development of a new experimentally verified advanced USI-SF system, representing qualitative seismic upgrading of isolated bridges with innovative SF energy dissipation devices. The analytical study presented in this paper actually is experimentally validated by respective quasi-static tests of newly designed seismic isolation and energy dissipation devices, and by complex shaking table tests of a constructed large-scale bridge prototype model with new advanced USI-SF system. Seismic protection advances of the USI-SF system are shown, and development of a new classically isolated as well as classical bridge model prototype is presented. With structural generalization of SF-ED devices, technological options applicable

for qualitative upgrading of various types of isolated bridges are extended.

2. Scope of present study

This paper presents results from the extended research devoted to development of advanced technology for seismic upgrading of isolated bridges with SF-ED devices. The paper is divided into two specific study parts. The first part of the paper contains results obtained by specific theoretical investigations of the hysteretic behaviour characteristics of the proposed structurally new types of SF-ED devices, Section 3. The refined 3D nonlinear analytical model applied in the paper was previously experimentally verified based on the results obtained via original nonlinear quasi-static tests on the constructed SF-ED prototype models under simulated repeated cyclic loads up to their induced deep nonlinearity. The second part of the study is based on the results of a previous extensive original experimental investigation, including the results of the nonlinear quasi-static tests of the new SF-ED devices and results of the successfully completed unique seismic shaking table tests of the constructed novel USI-SF bridge prototype model. The integral results were systematically presented, described, analysed and published, [23]. The study of results, and specific observations derived from the previously conducted experimental part of the study, enabled successful realization of the highly-significant extended complementary investigation, presented in this paper. The second part of the paper (sections 5, 6, 7 and 8) contains results of the investigations focusing on the theoretical analysis of seismic behaviour of bridges with the new USI-SF system, compared with common isolated systems and traditional (classical) structural systems under the effect of strong and very strong earthquakes. The formulated theoretical model was successfully verified using the results from the experimental shaking table tests of a single-span USI-SF bridge prototype model under strong earthquakes, with PGA of about 0.70 g. The verified model was further used theoretically to investigate seismic behaviour of the system under the effect of very strong earthquakes with PGA = 1.70 g, Section 5. The ensuing Section 6 presents modelling and comparative results of the earthquake response analyses of the common seismically isolated C-SI single-span bridge prototype model, model M1-A, in order to investigate the actual effect of the installed SF-ED devices. Then, using the experimentally verified concept, an adequate nonlinear theoretical model of a corresponding three-span USI-SF bridge prototype system was formulated and its realistic seismic behaviour was analysed for the effect of both strong and very strong earthquakes, Section 7. These investigations provided an insight into potential benefits of making a very important advancement of seismic protection of seismically isolated bridges against the effects of very strong earthquakes. Finally, the analysis of seismic behaviour of the same three-span bridge prototype model constructed by implementation of the traditional (classical) structural system was carried out to provide comparative results that will prove the stated advantages, Section 8.

3. Refined 3D hysteretic behaviour modelling of new types of SF-ED devices

The seismic energy dissipation system installed in the tested USI-SF bridge prototype model was composed of the newly developed basic type of SF energy dissipation device [23]. The main development steps for the new basic SF-ED-L1R device type, including design, production, testing as well as the final observations from the experimental hysteretic behaviour tests, were presented in the mentioned paper. The key objectives of the study were the following:

- The needed SF-ED devices of the proposed SF-ED-L1R type were not studied before and were not available on the market. Their original development included realization of a specific process, involving design of scaled prototype models of basic SF-ED-L1R device type, production of prototypes and their experimental testing for defining their actual hysteretic behaviour under the effect of earthquake like reversed cyclic loads.
- The present development of SF-ED prototype devices has not been limited to one basic device shape only. There is a possibility for their creative modification and creation of new important device shapes applicable in specific cases for seismic upgrading of bridges with different isolation systems.

Namely, three different shapes or types of SF-ED devices or systems are proposed in this paper:

- Type-1 of SF-ED devices formed with component width $L = 1R$ or SF-ED-L1R device, where R is radius of the component curvature;
- Type-2 of SF-ED devices formed with component width $L = 2R$ or SF-ED-L2R device;
- Type-3 of SF-ED devices formed with component width $L = 3R$ or SF-ED-L3R device.

Previous basic part of the research [23], including development and testing of SF-ED device type-1, provided the following important benefits:

- full mastering of technology for the design, production and testing of SF-ED devices;
- defining the actual hysteretic behaviour in formulation of analytical models;
- confirmation of its adequacy for direct use in the constructed large-scale bridge prototype model for dynamic testing on seismic shaking table;
- creation of conditions for experimental validation of the basic type of the USI-SF device.

This paper presents new results obtained by extended comparative research devoted to refined hysteretic behaviour modelling

and analytical hysteretic behaviour study of three proposed types of SF-ED devices capable of efficient seismic upgrading of isolated bridges exposed to strongest earthquake excitations. A refined 3D analytical model formulated by using ANSYS computer software [24] was implemented for numerical simulation of the hysteretic response of the new types of SF-ED devices. The advanced, experimentally verified refined nonlinear 3D modelling concept described in [23], has been consistently and successfully implemented for realization of the present extended study.

3.1. Hysteretic behaviour modelling of basic type-1 of SF-ED prototype models M11 and M12

The basic type-1 of SF-ED devices is characterized by a specific geometrical extension of the installed ED components, $L = 1R$, in horizontal direction considering from the fixation cross-section. If this horizontal extension of the device components L is known, then there is an additional possibility to assume assembling the device as complete with all eight components and as partial device, with four components. However, there is an additional possibility to design components with different cross-section properties and with different kind of ductile steel material. In the present study, the same cross-section geometry T1 was considered for all components, $b/h = 40 \text{ mm}/10 \text{ mm}$, for all three studied types of the novel SF-ED devices characterized by the use of three different shapes of ED components in the form of space flanges. In all three cases, in addition to complete device, the assembled partial devices composed of four ED components are also comparatively analysed. The adoption of this concept ensured very favourable conditions for comparative study of the realistic hysteretic behaviour characteristics of the three different types of devices, each assembled in two different structural options, under analytically simulated cyclic loads up to their deep nonlinearity.

Figure 1 shows the assembled basic type-1 of SF-ED devices. The first device is composed of eight ED components, model M11, representing the SF-ED-8C-L1R-T1 device, while the second consists of four ED components, model M12, representing the SF-ED-4C-L1R-T1 device.

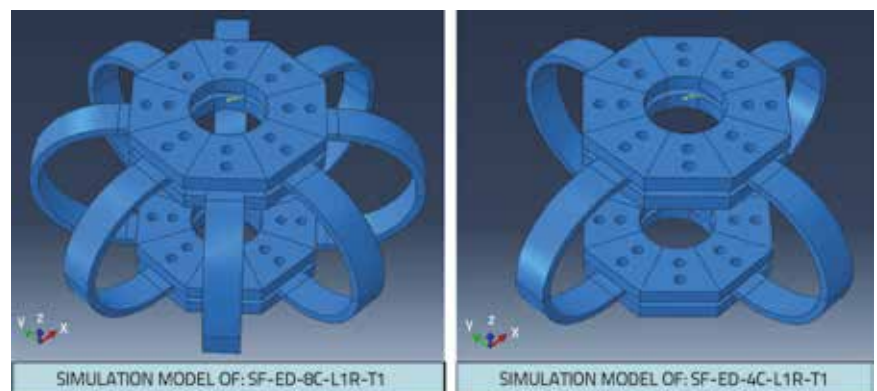


Figure 1. Assembled basic type-1 of SF-ED prototype devices composed of eight and four ED components representing M11 and M12 prototype models

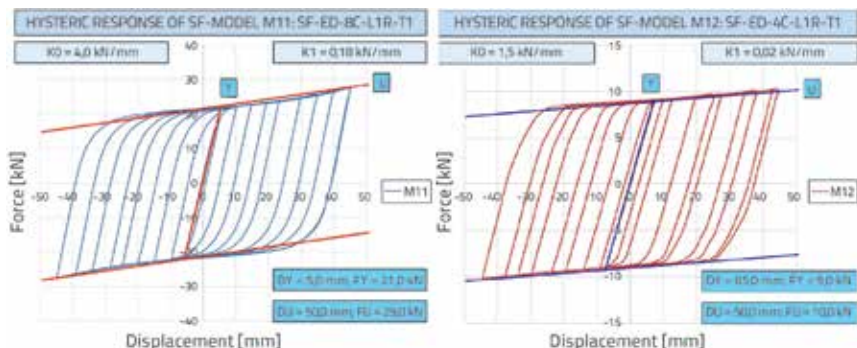


Figure 2. Computed hysteretic response under cyclic loads of basic type-1 of SF-ED prototype devices composed of eight and four ED components, representing M11 and M12 models

Table 1. Hysteretic behaviour properties of SF-ED-M11 and SF-ED-M12 devices computed using the nonlinear FEM model and simulated cyclic displacements with increasing amplitudes

No.	SF-ED Device M11: SF-ED-8C-L1R-T1			SF-ED Device M12: SF-ED-4C-L1R-T1		
	Notation	FEM model	[%]	Notation	FEM model	Δ [%]
1	DY [mm]	5.0	100.0	DY [mm]	6.0	120.0
2	FY [kN]	21.0	100.0	FY [kN]	9.0	42.8
3	KO [kN/mm]	4.0	100.0	KO [kN/mm]	1.5	37.5
4	K1 [kN/mm]	0.18	100.0	K1 [kN/mm]	0.02	11.1
5	K1/KO	0.045	100.0	K1/KO	0.013	28.8

Using the experimentally verified refined nonlinear 3D analytical models, the hysteretic responses of both prototype devices (models) under cyclic loads were successfully computed and presented comparatively in Figure 2. The computed results clearly indicate that the adopted representative bilinear analytical model can be implemented to realistically model the full hysteretic behaviour of the device. The defined parameters of the representative bilinear models are comparatively presented in Table 1. The following observations can be made regarding the partial device composed of four ED components, as compared to the full device composed of eight ED components:

- The yield displacement does not change significantly;
- The yield force is reduced to 42.8%, initial stiffness is reduced to 37.5% and the secant stiffness is reduced to 11.1%;
- The values of the representative K1/KO ratio amount to 4.5% and 1.3%, respectively.

This analysis directly confirmed that control of hysteretic behaviour

characteristics of the basic device type-1 can be predefined during the design process, taking into account actual design requirements.

3.2. Modelling hysteretic behaviour of created SF-ED type-2 of prototype models M21 and M22

The created type-2 of SF-ED device is characterized by specific geometrical extension of the installed ED components, $L = 2R$, in horizontal direction, considering the distance between the fixation cross-sections of the ED component.

Figure 3 shows the assembled type-2 of SF-ED devices. The left prototype composed of eight ED components represents SF-ED-8C-L2R-T1 device model M21, while the right SF-ED-4C-L2R-T1 prototype device having four ED components represents model M22. Using the formulated refined nonlinear

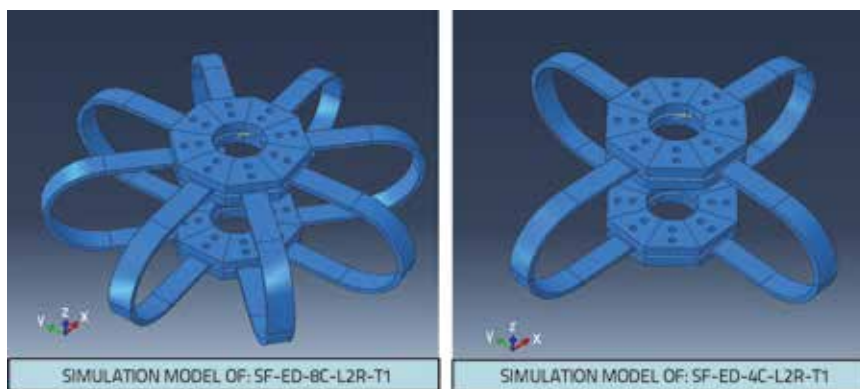


Figure 3. Created type-2 of SF-ED prototype devices composed of eight and four ED components representing M21 and M22 prototype models

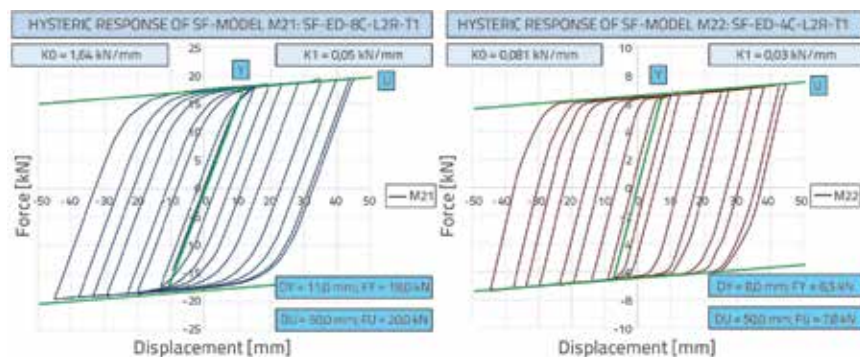


Figure 4. Computed hysteretic response under cyclic loads of basic type-2 of SF-ED prototype devices composed of eight and four ED components, representing M21 and M22 models

Table 2. Hysteretic behaviour properties of SF-ED-M21 and SF-ED-M22 devices computed using nonlinear FEM model and simulated cyclic displacements with increasing amplitudes

No.	SF-ED Device M21: SF-ED-8C-L2R-T1			SF-ED Device M22: SF-ED-4C-L2R-T1		
	Notation	FEM model	[%]	Notation	FEM model	Δ [%]
1	DY [mm]	11.0	100.0	DY [mm]	8.0	72.7
2	FY [kN]	18.0	100.0	FY [kN]	6.5	36.1
3	K0 [kN/mm]	1.64	100.0	K0 [kN/mm]	0.81	49.3
4	K1 [kN/mm]	0.05	100.0	K1 [kN/mm]	0.03	60.0
5	K1/K0	0.030	100.0	K1/K0	0.037	123.3

analytical model based on application of the same modelling concept, representative hysteretic behaviour curves were computed under simulated cyclic loads with increasing amplitudes up to deep nonlinearity, Figure 4.

The defined parameters of representative hysteretic bilinear models are given in Table 2. Compared to the first full device (prototype M21), significantly different hysteretic response parameters were obtained for the second partial device (prototype model M22):

- the yield displacement is reduced to 72.7 %;
- the yield force is reduced to 36.1 %;
- the initial stiffness K0 is reduced to 49.3 %;
- the values of the representative K1/K0 ratio amount to 3.0 % and 3.7 %, respectively.

This analysis also directly confirms that the required hysteretic behaviour characteristics can be effectively assured during the actual refined design analysis process.

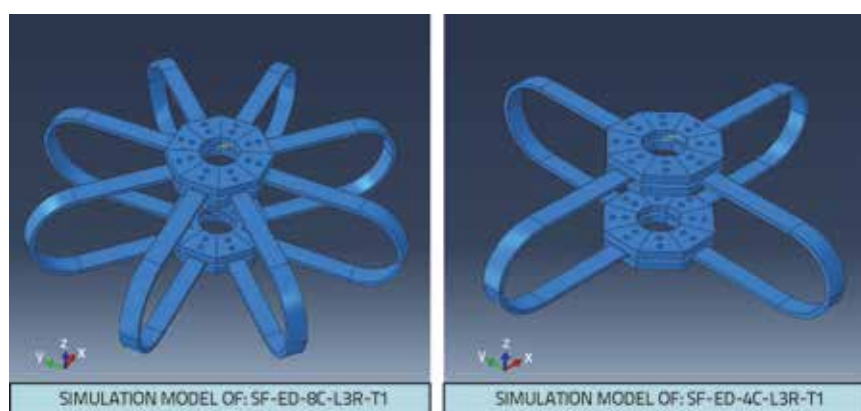
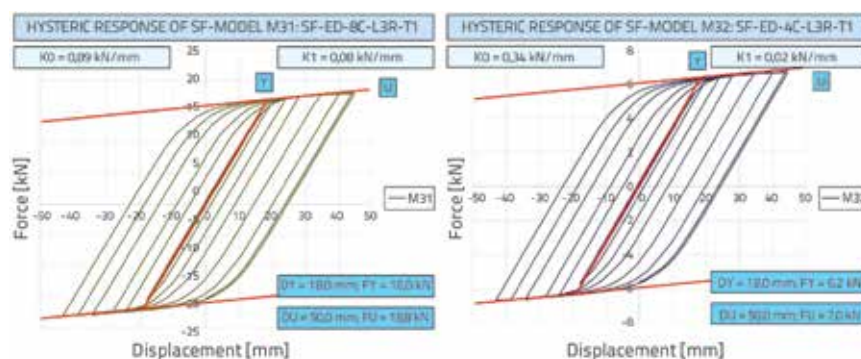
3.3. Hysteretic behaviour modelling of created SF-ED type-3 of prototype models M31 and M32

The created type-3 of SF-ED devices is characterized by specific geometrical extension of the installed ED components $L = 3R$, in horizontal direction, considering the distance between the fixation cross-sections of the ED component.

Figure 5 shows the assembled type-3 of SF-ED devices. The first (left-side) device

is composed of eight ED components representing the SF-ED-8C-L3R-T1 device prototype model M31, while the second (right-side) device SF-ED-4C-L3R-T1 is composed of four ED components, representing the prototype model M32.

Using also the formulated respective nonlinear 3D analytical models, the representative hysteretic behaviour curves were computed under simulated cyclic loads with increasing amplitudes up

**Figure 5. Created type-3 of SF-ED prototype devices composed of eight and four ED components, representing M31 and M32 prototype models****Figure 6. Computed hysteretic response under cyclic loads of basic type-3 of SF-ED prototype devices composed of eight and four ED components, representing M31 and M32 models****Table 3. Hysteretic behaviour properties of SF-ED-M31 and SF-ED-M32 devices computed using formulated nonlinear FEM model and simulated cyclic displacements with increasing amplitudes**

No.	SF-ED Device M31: SF-ED-8C-L3R-T1			SF-ED Device M32: SF-ED-4C-L3R-T1		
	Notation	FEM model	[%]	Notation	FEM model	Δ [%]
1	DY [mm]	18.0	100.0	DY [mm]	18.0	100.0
2	FY [kN]	16.0	100.0	FY [kN]	6.2	38.7
3	K0 [kN/mm]	0.89	100.0	K0 [kN/mm]	0.34	38.2
4	K1 [kN/mm]	0.08	100.0	K1 [kN/mm]	0.02	25.0
5	K1/K0	0.089	100.0	K1/K0	0.058	65.1

to deep nonlinearity, Figure 6. Parameters of the representative hysteretic bilinear models are given in Table 3.

In respect to the first complete prototype model M31, significantly different hysteretic response parameters were obtained for the second partial device prototype model M32:

- yield displacement was the same;
- yield force was reduced to 38.7 %;
- initial stiffness K_0 was reduced to 38.2 %;
- the values representing the K_1/K_0 ratio amounted to 8.9 % and 5.8 %, respectively.

Finally, it was also confirmed that the required hysteretic behaviour characteristics of this device type could be successfully defined during the formulated refined design analysis process.

3.4. Concluding Observations

Summarizing hysteretic behaviour results for three types of innovative SF-ED devices, the following concluding observations can be made:

- The basic type-1 of SF-ED devices in two options, SF-ED-8C-L1R-T1 and SF-ED-4C-L1R-T1, characterized by horizontal extension of the ED components $L = 1R$, can be efficiently used for seismic upgrading of isolated bridges, especially in the case of bridges with presently quite high seismic gap.
- Two new proposed types of SF-ED devices, type-2 with two options, SF-ED-8C-L2R-T1 and SF-ED-4C-L2R-T1, and type-3 with two options, SF-ED-8C-L3R-T1 and SF-ED-4C-L3R-T1, characterized by geometrical property of ED components with $L = 2R$ and $L = 3R$, respectively, can be efficiently used for seismic upgrading of isolated bridges with relatively smaller seismic gaps.
- Considering the same cross-sections of ED components, three different yield forces were recorded for the three different types of full SF-ED devices with 8 components, $F_{Y1} = 21.0$ kN, $F_{Y2} = 18.0$ kN (85.7 %) and $F_{Y3} = 16.0$ kN (76.2 %), for type-1, type-2 and type-3, respectively.
- The initial stiffness of the three types of SF-ED devices was also significantly reduced, becoming $K_{01} = 4.0$ kN/mm, $K_{02} = 1.64$ kN/mm (41.0 %) and $K_{03} = 0.89$ kN/mm (22.2 %).
- On the other hand, the actual yield displacements of the same three types of SF-ED devices increased significantly, becoming $F_{Y1} = 5.0$ mm, $F_{Y2} = 11.0$ mm (220 %) and $F_{Y3} = 18.0$ mm (360.0 %).
- Very similar tendency of hysteretic behaviour characteristics was observed regarding the analysed three types of reduced SF-ED devices, composed of four ED components.
- Consistently presented study results show that the introduced new types of SF-ED devices could be used as a reliable, adaptive and effective concept for efficient seismic upgrading of isolated highway bridges, especially for cases where very strong earthquake effects are expected.

4. USI-SF bridge prototype model used for shaking table tests

Dimensions of constituent elements of prototype bridge and their contribution to the actual bridge performance, characteristics of the main structural components, type of seismic isolation system implemented, and characteristics of the installed original SF-ED devices, were taken into account during design of the presently constructed and tested bridge prototype model, Figure 7.

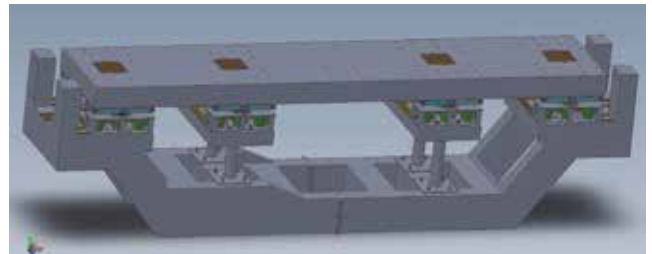


Figure 7. Designed large-scale USI-SF bridge prototype model tested on IZiIS seismic shaking table for validation of proposed technology and formulated nonlinear analytical model

Due to the size (5.0 m x 5.0 m) and payload capacity of the seismic shaking table, the basic ISUBBRIDGE model had to be geometrically reduced with respect to the selected prototype. From these reasons, the geometrical scale factor of 1:9 was adopted. It was used to verify the referred constraints in this case, but with the adopted specific model design concept. As a consequence of the scale reduction, the relevant properties involved in the dynamic tests were scaled according to the similitude law [25]. Considering the main related factors, an adequate combined true replica-artificial mass simulation model was adopted. For simulation of the stiff RC superstructure, a stiff slab with added mass was adopted using the same material as that of the prototype structure. Steel material was used for simulation of central piers. The seismic isolation and energy dissipation devices were designed and produced in reduced scale. The similitude law implies the adopted relations for the different parameters, all given in terms of the geometrical scale factor (lr). Concrete material type C25/30 was used for the construction of RC segments of the bridge model, while steel material type S355 was selected and applied for construction of steel SF-ED devices. Considering the above design parameters, the experimental model of the bridge was primarily conceptualized so as to create best possible realistic conditions for successful fulfilment of main research objectives defined and studied in the frame of the present research, [26-29]. It includes original experimental validation of actual seismic performances of the USI-SF system under the effects of very strong earthquake excitations. To meet the stated objectives, a large-scale physical model of a typical three-span prototype bridge was constructed and used for shaking table tests [23], Figure 8, Figure 9, and Figure 10.



Figure 8. Manufacturing RC continuous slab representing bridge superstructure



Figure 9. Concreted left RC substructure segment of designed USI-SF bridge prototype model



Figure 10. Large-scale USI-SF bridge prototype model used for shaking table tests under simulated strong earthquakes: (1) left end support; (2) right end support; (3) support above shorter central piers; (4) support above longer central piers

The substructure of the prototype-bridge experimental model is composed of two parallel rigid RC beams with an appropriate inclination at both ends to provide for an elevated horizontal positioning of abutment supports. Horizontal parts of both

parallel RC beams are used for resting the bridge model on the seismic shaking table in the direction of its diagonal. The total length of horizontal part of the RC beams is $l_1 = 520.0$ cm. The inclined parts of both ends with their extensions amount to: $l_2(\text{left}) = l_2(\text{right}) = 155.0$ cm. With these dimensions, the total length of the substructure amounts to $L_{DS} = 520.0 + 2 \cdot 155.0 = 830.0$ cm. The two parallel beams are constructed to have a cross-section of $b/h = 25$ cm/50 cm. However, on the left side, the height of cross-section is increased by 20.0 cm, amounting to $b/h = 25$ cm/70 cm. In this way, the condition for building central piers of different heights is fulfilled. Both parallel RC beams are mutually connected by six transverse RC beams, three on each half.

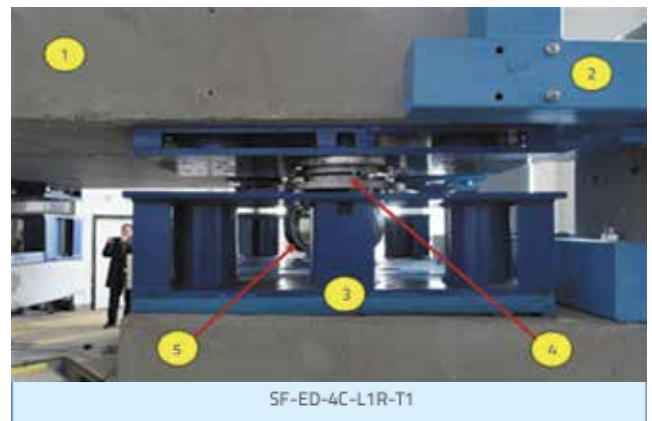


Figure 11. Detail of new devices for testing: (1) superstructure; (2) steel support of DL-device; (3) steel support of DSRSB device; (4) DSRSB device; (5) SF-ED-4C-L1R-T1 device

Central piers are constructed in pairs of two steel-made piers of hollow circular cross-section, $D = 168$ mm in diameter, and $t = 12.0$ mm in wall thickness. On the upper surface, the steel piers have steel connecting end plates that support RC bent slabs measuring 90 cm \times 150 cm \times 20 cm. On the RC bent slabs, two symmetrical positions are provided for optional installation of a pair of DSRSB devices, with SF-ED devices positioned between them. The entire substructure is precast and is composed of two parts of identical length (Figure 7 and Figure 10).

The superstructure of the prototype bridge model is constructed as a RC deck slab of necessary weight (Figure 7 and Figure 10). To ensure this necessary weight, the RC slab is realised with cross-sectional dimensions of $b/d = 150/30$ cm. The total length of the RC slab is $l = 740.0$ cm. A free space of $D_1 = D_2 = 20$ cm is left at each end. Located further, there are vertical cantilever end columns $b_1 = b_2 = 25.0$ cm in width. Again, considering the dimensions at the top level, the total length of the entire experimental bridge model is $L = 740.0$ cm $+$ $2 \cdot 20.0$ cm $+$ $2 \cdot 25.0$ cm $= 830.0$ cm. The RC slab is placed at a height distance of $h_d = 40.0$ cm from the highest RC substructure surfaces. This space (seismic gap) is used for the location of two (2) metal spacers at each supporting position (there are two end and two central supporting positions). DSRSB devices are mounted on

these metal spacers while, between the metal spacers, there is a space for the installation of novel SF-ED devices, Figure 11.

5. Modelling and earthquake response characteristics of the tested USI-SF single-span bridge prototype model M1

Experimental results obtained for the large scale USI-SF single-span bridge prototype model M1 tested on the seismic shaking table under simulated strong real earthquakes were successfully used in these investigations for the following purposes:

- to enable reliable verification of the analytical model;
- to use the experimentally verified theoretical model to investigate real behaviour of the new single-span USI-SF bridge system under the effects of very strong earthquakes;
- to use the experimentally verified theoretical model to comparatively investigate real behaviour of the same scaled model composed as common seismically isolated C-SI single-span bridge system under the same earthquake effects;
- to prove applicability of the analytical model in the study of seismic behaviour of the assembled large-scale three-span USI-SF bridge system.

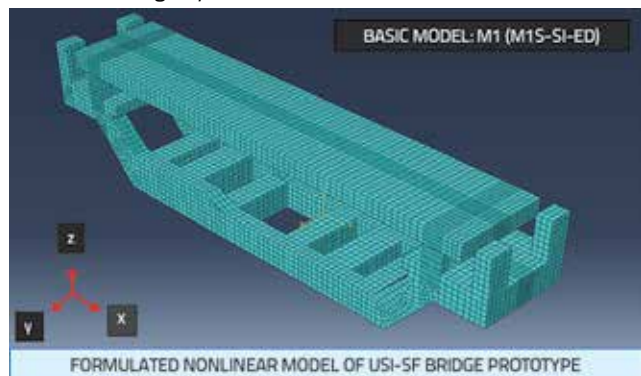


Figure 12. Formulated nonlinear analytical model of the tested large-scale USI-SF bridge prototype model used for realization of the present analytical study

The analytical nonlinear model of the tested large-scale single-span USI-SF bridge prototype model M1, Figure 12, was formulated using the same geometry and results available from the previously performed experimental investigations of hysteretic behaviour of main nonlinear components of the bridge system, Figure 13. Two identical seismic bearings of the DSRSB type, marked by 1, 2 and 3, 4, were installed at the left and right abutment, respectively. New seismic energy dissipation devices of the SF-ED type were installed between them, each with four ED components indicated as A and B, respectively. Four components are needed to provide for adequate mechanical properties for the conducted experimental tests. Thus, they are properly included in the formulated analytical model. Experimental investigations proved that the hysteretic behaviour of the DSRSB devices can

be very successfully simulated by a bilinear hysteretic model defined with two points, namely, yielding point-Y and point-U by which the slope of the second rule is defined. The following deformations and forces for the corresponding bilinear model of DSRSB devices were defined by experimental testing: $D_y = 1.0 \text{ mm}$; $F_y = 0.3 \text{ kN}$; $D_u = 50.0 \text{ mm}$; $F_u = 0.9 \text{ kN}$. Analogously, the experimental investigations proved that the hysteretic behaviour of the new SF-ED devices of type-1 can also be very successfully simulated by a corresponding bilinear model. The following parameters of the representative bilinear model of SF-ED devices with four ED components were defined with the experimental investigations: $D_y = 6.0 \text{ mm}$; $F_y = 9.0 \text{ kN}$; $D_u = 50.0 \text{ mm}$; $F_u = 10.0 \text{ kN}$. The realistic behaviour of the RC substructure and the superstructure of the constructed and tested bridge prototype model-M1 was very accurately simulated analytically in SAP2000 by a refined mesh of 3D solid linear finite elements (892 in total), representing very stiff respective RC segments, Figure 12. The respective nonlinear behaviour of the tested DSRSB and SF-ED devices was very successfully simulated analytically by the existing nonlinear link elements. The initial verification of the realized level of similarity between the designed and the constructed bridge prototype model M1 was performed through comparison of dynamic characteristics of the partial system with only four DSRSB devices installed, without SF-ED devices being present. For such partial bridge system, two fundamental theoretically computed periods of vibration amounted to $T_1 = T_2 = 0.500 \text{ s}$, while the experimentally defined values by vibration sine-sweep test are quite close and amount to $T_1 = 0.522 \text{ s}$ and $T_2 = 0.521 \text{ s}$, Table 4.

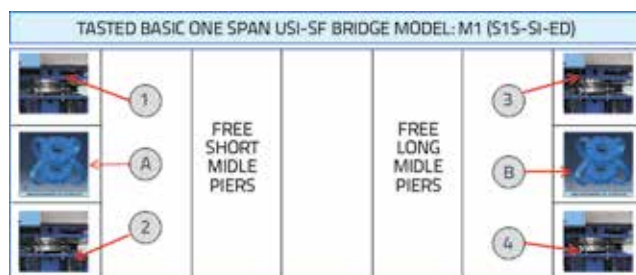


Figure 13. Positions of DSRSB and SF-ED devices of the tested one-span large-scale USI-SF bridge prototype model M1 on seismic shaking table

Confirmation of successful use of the formulated analytical model for the purposes of this study is made by comparing dynamic characteristics of the composed complete bridge prototype model with the installed DSRSB and SF-ED devices. Dynamic characteristics of the complete bridge prototype model defined experimentally by a vibration sine-sweep test, and those obtained theoretically using the formulated analytical model, are very close amounting respectively to $T_1 = 0.348 \text{ s}$; $T_2 = 0.347 \text{ s}$ and $T_1 = 0.347 \text{ s}$; $T_2 = 0.346 \text{ s}$, which is a negligible difference, Table 4. Actually, the obtained difference is only 0.3 % and shows that the formulated analytical model

Table 4. Validation of USI-SF analytical model M1 based on computed dynamic characteristics

Fundamental periods of the tested USI-SF bridge model M1 (I. Bridge model with DSRSB devices only-experimental: T1 = 0.522 s; T2 = 0.521 s)					
II. Bridge model with DSRSB and SF-ED devices					
Experimental (sine-sweep)			Theoretical (3D model)		
1	T1 = 0.348 s	100 %	1	T1 = 0.347 s	-0.3 %
2	T2 = 0.347 s	100 %	2	T2 = 0.346 s	-0.3 %

Table 5. Validation of USI-SF analytical model M1 based on shaking table tests results

Seismic response of the tested USI-SF bridge model M1 (Relative displacement of bridge superstructure in shaking table direction: peak average)					
EI Centro earthquake: PGA = 0,77 g					
Experimental (2 channels)			Theoretical (Nonlinear 3D Model)		
1E	Dmax = 21.57 mm	100 %	1T	Dmax = 23.97 mm	+11.1 %
Petrovac earthquake: PGA = 0,71 g					
Experimental (2 channels)			Theoretical (Nonlinear 3D Model)		
2E	Dmax = 17.57 mm	100 %	2T	Dmax = 19.03 mm	+8.3 %

Table 6. Computed γ -components of positive and negative values of selected characteristic parameters of USI-SF bridge model M1 for two intensity levels of EI Centro and Petrovac earthquakes

No.	Earthquake level-1: EI Centro PGA = 0,77 g			Earthquake level-2: EI Centro PGA = 1,7 g		
	Notation	Max (+)	Max (-)	Notation	Max (+)	Max (-)
1	DYmax [mm]	17.0	15.0	DYmax [mm]	33.0	24.0
No.	Earthquake level-1: Petrovac PGA = 0,71 g			Earthquake level-2: Petrovac PGA = 1,7 g		
	Notation	Max (+)	Max (-)	Notation	MaxD (+)	MaxD (-)
1	DYmax [mm]	16.0	11.0	DYmax [mm]	29.0	34.0

can be regarded as highly realistic for the initial state of the USI-SF bridge system, and that it meets conditions for realistic simulation study.

The second most important step in verification of the formulated analytical model was realized through the experimental seismic response results recorded during complex seismic shaking table tests of the constructed complete single-span, large-scale, USI-SF bridge prototype model under simulated effects of strong earthquakes. As the most important control parameters, the maximum displacements of the superstructure recorded during experimental tests were compared to those computed theoretically using the formulated nonlinear analytical model, Table 5. Under the effect of the simulated strong earthquake EI Centro with PGA = 0.77 g, the defined average peak displacement from four recorded peaks during the experiment amounted to Dmax = 21.57 mm, while the same displacement obtained by theoretical analysis with reference to the same conditions amounted to Dmax = 23.97 mm. Similarly, under the effect of the simulated strong earthquake Petrovac with PGA = 0.71 g, the defined average peak displacement

from four recorded peaks during the experiment amounted to Dmax = 17.57 mm, whereas that obtained from the theoretical analysis amounted to Dmax = 19.03 mm. The obtained difference in the first case amounted to only 11.1 %, whereas in the second case, it was even smaller, amounting to only 8.3 %, Table 5. The presented comparative results obtained by experimental testing of the large-scale, single-span USI-SF bridge prototype model, and theoretical results obtained by application of the formulated nonlinear analytical model, point out that the applied analytical model formulated on the basis of experimentally proved parameters of nonlinear behaviour of built-in devices can be used very successfully for realistic simulation of complex nonlinear behaviour of composed innovative bridge systems by incorporation of seismic isolation systems and new SF-ED seismic energy dissipation devices. Due to the capacity of the seismic shaking table and the considerable weight of the constructed large-scale USI-SF bridge prototype model, it was not possible to simulate earthquakes stronger than the stated ones. However, within the frames of the considered study, a great interest was shown as to the exploration of the real behaviour of the innovative USI-SF bridge protection system under much stronger earthquakes. A complete and very realistic

simulation record of the presented complex problem was obtained by theoretical analysis of the seismic response of the composed full USI-SF system under simulated effect of much stronger EI Centro and Petrovac earthquakes defined by peak accelerations of as many as PGA = 1.70 g.

The anticipated analysis was conducted quite successfully. The most characteristic comparative results referring to the effect of strong and very strong earthquakes are presented in Figure 14, Figure 15, Figure 16, and Table 6. These three figures graphically show the selected most important comparative results obtained from two analyses conducted to simulate the effects of strong and very strong EI Centro earthquake, as representative examples. Similar response properties are obtained from two respective analyses simulating two intensities of Petrovac earthquake. Figure 14 shows the representative hysteretic response in γ -direction of DSRSB type seismic bearing located on the left side, under the effect of EI Centro earthquake scaled to PGA = 0.77 g and PGA = 1.70 g.

Figure 15 comparatively presents computed hysteretic responses of the new SF-ED-4C-L1R-T1 energy dissipation

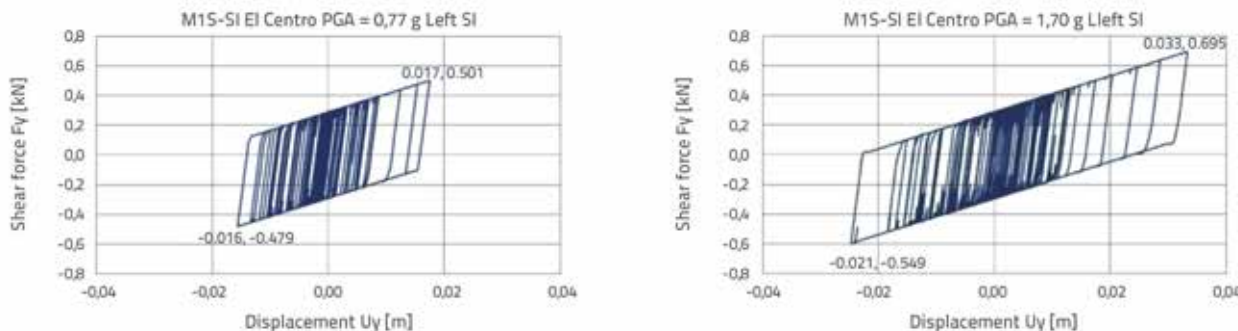


Figure 14. USI-SF bridge model M1: Hysteretic F-D response in y-direction of the left DRSB device under El Centro earthquake scaled to PGA = 0.77 g and PGA = 1.70 g in shaking table direction

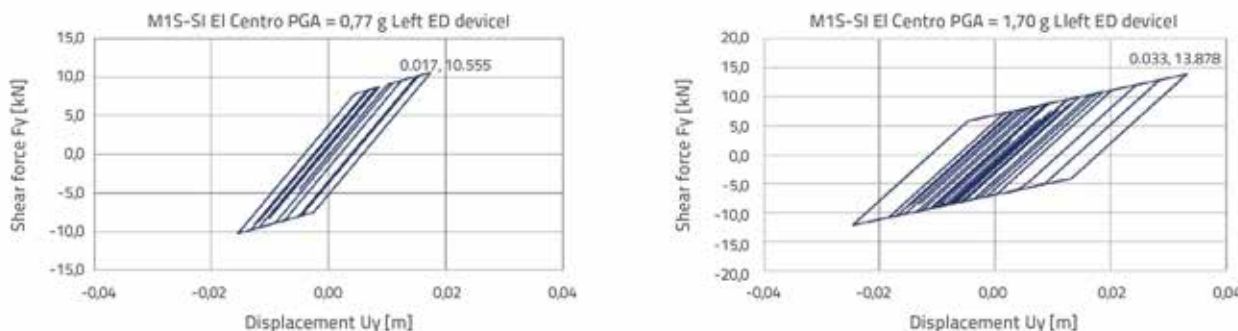


Figure 15. USI-SF bridge model M1: Hysteretic F-D response in y-direction of the left SF-ED device under El Centro earthquake scaled to PGA = 0.77 g and PGA = 1.70 g in shaking table direction

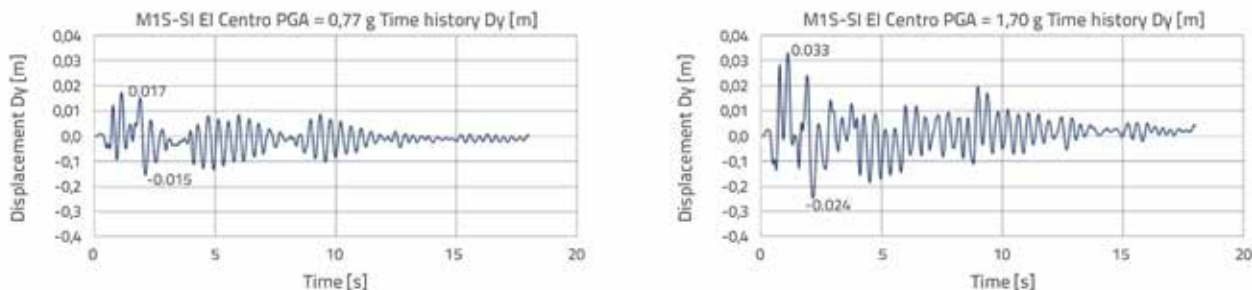


Figure 16. USI-SF bridge model M1: Displacement response in y-direction DY under El Centro earthquake scaled to PGA = 0.77 g and PGA = 1.70 g in shaking table direction

device in y-direction under the simulated El Centro earthquake scaled to PGA = 0.77 g and PGA = 1.70 g, respectively. Analogously, Figure 16 comparatively presents computed relative displacement responses of the superstructure in y-direction under simulated effect of the real time compressed El Centro earthquake scaled to both stated intensities representing strong and very strong earthquake action. Finally, Table 6 comparatively shows, for the two earthquake intensities, the computed y-components of the positive and negative peaks or maximum relative displacements of bridge model superstructure. Considering the computed results, which clearly demonstrate very consistent insight into the complete seismic behaviour characteristics of the new USI-SF single-span bridge prototype system, the following important conclusions can be made:

- The formulated nonlinear analytical model of the new USI-SF bridge system enabled very successful simulation of the actual experimentally recorded seismic response of the tested large-scale prototype model under simulated strong earthquake effects on seismic shaking table;
- The above observations reveal that the presently formulated experimentally confirmed nonlinear analytical modelling concept provided was a successful realization of the above presented highly important “analytical seismic test” of the new USI-SF bridge prototype model under simulated very strong earthquakes represented by PGA = 1.70 g. The USI-SF nonlinear model behaviour study, planned to be realized with specified very special experimental testing conditions, was out of the shaking table working capability and, consequently, its realization in the laboratory shaking table proved impossible;

- The obtained research results show that the proposed new USI-SF seismic protection system for seismic upgrading of isolated bridges possesses a pronounced stability and functioning capability even under the effect of very strong repeated earthquakes. Generally, the functioning capability depends on the efficiency of the implemented pre-defined concept for avoiding problems resulting from permanent deformations. Possible permanent deformation can be accommodated with specific structure of the installed expansion joints and/ or by post earthquake intervention to eliminate permanent displacements using special force application devices developed for such specific purposes.

6. Modelling and comparative earthquake response analysis of common seismically isolated C-SI single-span bridge prototype model M1-A

The modelling and comparative earthquake response analysis of the assembled common seismically isolated C-SI single-span bridge prototype model M1-A was carried out specifically in order to investigate the potential upgrading level of the presently introduced innovative SF-ED devices. The respective analytical nonlinear model M1-A was formulated based on an already implemented analogous concept. However, the two SF-ED devices were removed. At the same positions, only four identical seismic bearings of the DSRSB type were considered, i.e. 1, 2 and 3, 4, on the left and the right abutment, Figure 17. Other parameters of the analytical model were considered to be identical.

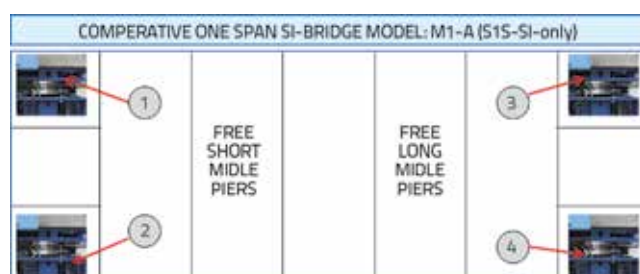


Figure 17. Positions of DSRSB devices of the analysed common seismically isolated C-SI single-span bridge prototype model M1-A (M1S-SI-only)

Considering the defined C-SI model configuration, the seismic response was analysed for all four selected representative analysis cases, simulating the same two intensities of El Centro earthquake scaled to $PGA = 0.77\text{ g}$ and $PGA = 1.70\text{ g}$, and two intensities of Petrovac earthquakes scaled to $PGA = 0.71\text{ g}$ and $PGA = 1.70\text{ g}$. Comparatively, Table 7 shows computed y -components of positive and negative peaks or maximum relative displacements of bridge model superstructure for the two

Table 7. Computed y -components of superstructure positive and negative peak relative displacements of the assembled common seismically isolated C-SI bridge prototype model M1-A for two intensity levels of El Centro and Petrovac earthquakes

No.	Earthquake level-1: El Centro $PGA = 0,77\text{ g}$			Earthquake level-2: El Centro $PGA = 1,7\text{ g}$		
	Notation	Max (+)	Max (-)	Notation	Max (+)	Max (-)
1	DYmax [mm]	(17,0) / 13,6	(15,0) / 30,8	DYmax [mm]	(33,0) / 44,4	(24,0) / 67,1
No.	Earthquake level-1: Petrovac $PGA = 0,71\text{ g}$			Earthquake level-2: Petrovac $PGA = 1,7\text{ g}$		
	Notation	Max (+)	Max (-)	Notation	MaxD (+)	MaxD (-)
1	DYmax [mm]	(16,0) / 20,7	(11,0) / 7,6	DYmax [mm]	(29,0) / 39,9	(34,0) / 18,3

earthquake intensities, and for the two different bridge model configurations. The computed relative peak displacements of the superstructure of the assembled common seismically isolated C-SI single-span bridge prototype model M1-A (without SF-ED devices) are much larger than peak displacements obtained for the assembled new USI-SF bridge prototype model configuration (shown comparatively in parentheses). The presented results clearly demonstrate great importance of the implemented SF-ED devices for the seismic upgrading of isolated bridges. For example, the maximum relative displacement amounted to $D_{max} = 67.1\text{ mm}$ for the simulated very strong earthquake El Centro represented with $PGA = 1.70\text{ g}$.

Such large resulting displacement is critical and will cause total failure of the prototype bridge superstructure, since the displacement limit of DSRSB devices amounts to $D_a = 40.0\text{ mm}$. However, with incorporation of SF-ED devices, maximum relative displacement was significantly reduced to $D_{max} = 33.0\text{ mm}$. However, it is particularly important to point out that such great reduction of relative displacement, amounting to 103.3 %, was recorded in the case of the strongest earthquake intensity. Research results obtained in this part of the study show that the proposed new USI-SF seismic protection system possesses pronounced capability for seismic upgrading of isolated bridges, which is particularly important for the effect of future very strong earthquakes.

7. Modelling and earthquake response characteristics of assembled USI-SF three-span bridge prototype model M2

The refined nonlinear theoretical model of comparatively assembled three-span USI-SF bridge prototype model M2 was formulated in SAP2000, [30, 31], by applying the knowledge gained from the above presented studies and the capability of the experimentally verified modelling concept of the new system. Using the formulated experimentally verified analytical model, the seismic behaviour analysis of the assembled comparative three-span USI-SF bridge system was carried out for the effect of strong and very strong earthquakes, actually representing a reliable "analytical experiment". The assembled three-span USI-SF bridge prototype system contains a characteristic variant of distribution of seismic isolation devices and new seismic energy dissipation devices, Figure 18. The same seismic bearings of DSRSB type were installed on all four supports, namely, two

seismic bearings on the left abutment and two seismic bearings on the right abutment, indicated by 1, 2 and 3, 4, respectively, and also two seismic bearings over the left (shorter) central piers and two seismic bearings over the right (longer) central piers, indicated by 5, 6 and 7, 8, respectively.

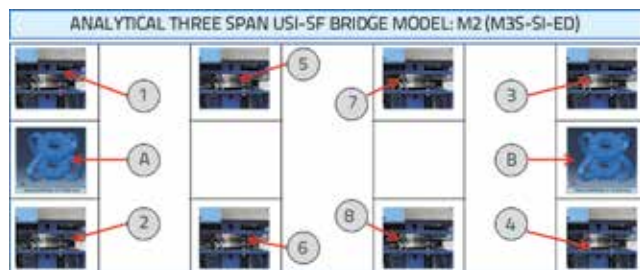


Figure 18. Positions of DSRSB and SF-ED devices of the assembled three-span large-scale USI-SF bridge prototype model M2

The tested SF-ED-4C-L1R-T1 energy dissipation devices were installed only on the left and right-side abutments, between seismic bearings, indicated by A and B, respectively. The hysteretic characteristics of the considered seismic bearings and seismic energy dissipation devices were kept identical to those used in the case of the previous experimentally tested large-scale USI-SF single-span bridge prototype model M1. The nonlinear analytical model of the newly assembled three-span bridge prototype system M2 applied in the considered analyses was formulated analogously to the previous one adopting 1893 nodal points.

However, in this case, the existing shorter and longer central piers, composed of metal tube-like profiles with a circular cross-section, were integrated into the model with 104 frame elements. The model included 892 elastic solid elements, 40 elastic shell elements for modelling caps above shorter and longer piers, 10 nonlinear link elements, and 136 restraints. Concrete material type C25/30 and steel material type S355 were considered. In the analytical model, the central piers were treated as linear elements to provide a direct insight into seismic behaviour of the installed DSRSB and SF-ED devices. Analogously, in this case, the analyses of seismic response of the system to the effect of both earthquakes scaled to the level of strong and very strong earthquake were performed. The scaled peak acceleration of the El Centro earthquake for the strong and very strong earthquake amounted to $PGA = 0.77\text{ g}$ and $PGA = 1.70\text{ g}$, whereas in the case of the Petrovac earthquake, these amounted to $PGA = 0.71\text{ g}$ and $PGA = 1.70\text{ g}$, respectively. The most characteristic results are selected out of the set of performed analyses and presented in Figure 19, Figure 20, Figure 21, Figure 22, and Figure 23. Figure 19 comparatively shows hysteretic responses of DSRSB device 1 in y-direction, obtained under the effect of El Centro earthquake scaled to $PGA = 0.77\text{ g}$ and $PGA = 1.70\text{ g}$, respectively. The presented plots show that a very stable cyclic behaviour of the modelled DSRSB devices is exhibited in both cases whereas, in the second case, considerably larger relative peak displacements of the superstructure are evident. Analogously, hysteretic responses of the SF-ED-4C-L1R-T1 energy dissipation device

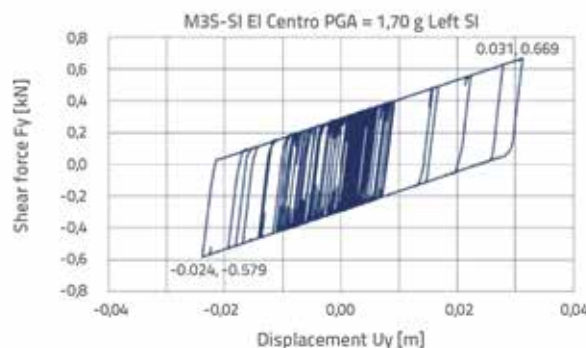
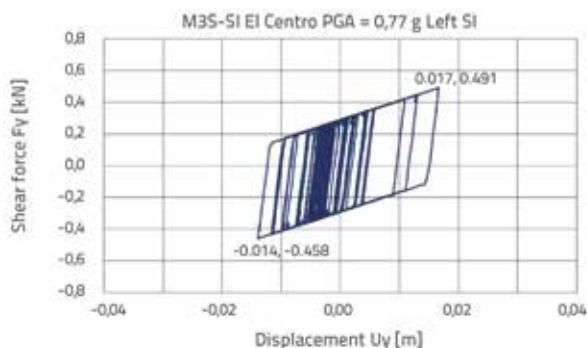


Figure 19. USI-SF bridge model M2: Hysteretic F-D response in y-direction of the left DSRSB device under El Centro earthquake scaled to $PGA = 0.77\text{ g}$ and $PGA = 1.70\text{ g}$ in shaking table direction

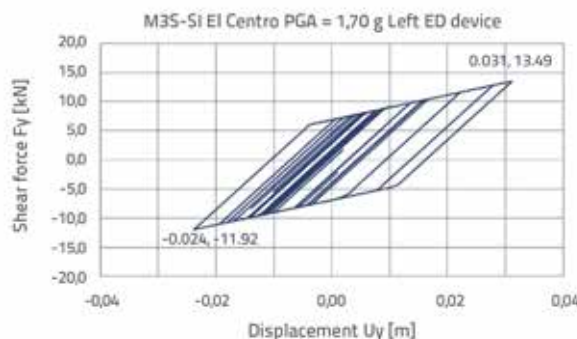
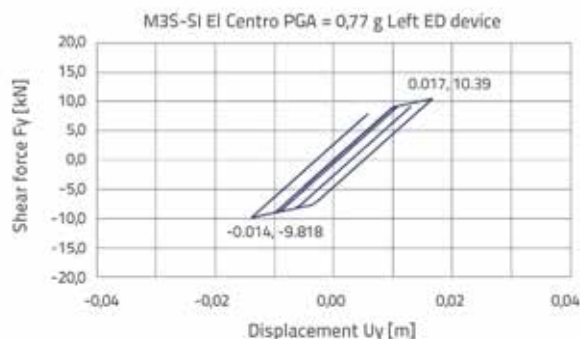


Figure 20. USI-SF bridge model M2: Hysteretic F-D response in y-direction of the left SF-ED device under El Centro earthquake scaled to $PGA = 0.77\text{ g}$ and $PGA = 1.70\text{ g}$ in shaking table direction

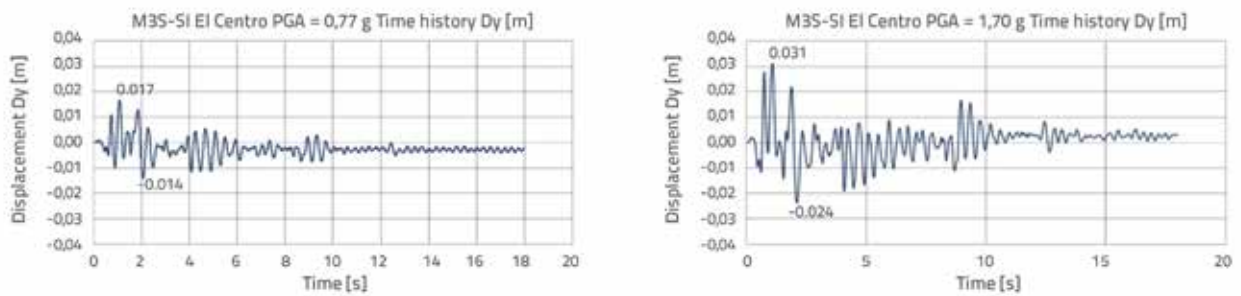


Figure 21. USI-SF bridge model M2: Displacement response in y-direction DY under El Centro earthquake scaled to PGA = 0.77 g and PGA = 1.70 g in shaking table direction

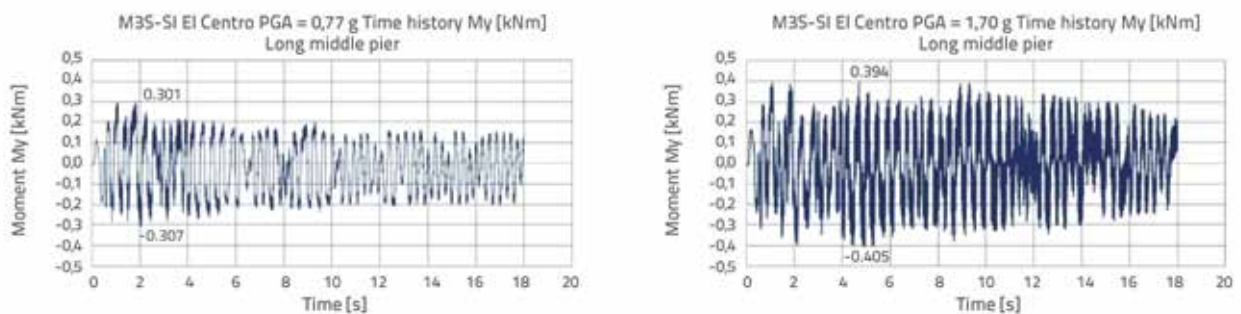


Figure 22. USI-SF bridge model M2: Moment response MY at fixed bottom point of long central pier under El Centro earthquake scaled to PGA = 0.77 g and PGA = 1.70 g in shaking table direction

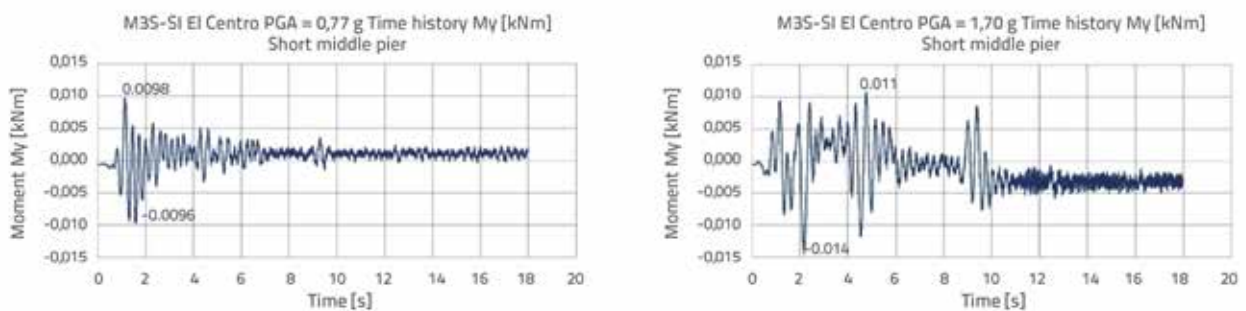


Figure 23. USI-SF bridge model M2: Moment response MY at fixed bottom point of short central pier under El Centro earthquake scaled to PGA = 0.77 g and PGA = 1.70 g in shaking table direction

A in y-direction are presented comparatively in Figure 20. Also, in this case, a more intense activation of the SF-ED device was recorded in the case of simulation of a higher-intensity earthquake. It is important to note that the maximum force activated at the DSRSB seismic bearing was much smaller, amounting to $\max F = 0.67$ kN, whereas, at the SF-ED-4C-L1R-T1 seismic energy dissipation device, it reached the value of $\max F = 13.49$ kN. These results point to a highly important positive role of the new SF-ED devices resulting in a favourable global seismic response modification. With large dissipation of seismic energy, a positive reduction of maximum relative displacements of the superstructure was successfully achieved. The stated tendency is also clearly presented in Figure 21, which provides a comparative presentation of time histories of relative displacements of the superstructure in y-direction under the effect of the El Centro earthquake. In case of a strong earthquake scaled to PGA = 0.77

g, the obtained maximum displacement in y-direction amounted to $\max Dy = 17.0$ mm, whereas the maximum displacement amounted to $Dy = 31.0$ mm under very strong earthquake scaled to PGA = 1.70 g, Table 8. In the same table, a similar tendency can be observed for the influence of the Petrovac earthquake. $\max Dx = 15.0$ mm was obtained under the Petrovac earthquake scaled to PGA = 0.71 g, whereas under the same earthquake scaled to a very strong intensity of PGA = 1.70 g, the maximum displacement amounted to $\max D = 34.0$ mm. Due to simulated earthquake action under an angle of 45° with respect to the longitudinal bridge axis, identical displacements in x and y direction were computed ($Dx = Dy$), representing component displacement values. Maximum displacements in the direction of earthquake action are higher and amount to $\max D = \sqrt{2} \cdot Dx = \sqrt{2} \cdot Dy$. The same relation also holds for all other computed component physical quantities. The applied concept of installation of seismic

Table 8. Computed γ -components of positive and negative values of selected characteristic parameters of USI-SF bridge model M2 for two intensity levels of El Centro and Petrovac earthquakes

No.	Earthquake level-1: El Centro PGA = 0,77 g			Earthquake level-2: El Centro PGA = 1,7 g		
	Notation	Max (+)	Max (-)	Notation	Max (+)	Max (-)
1	DYmax [mm]	17.0	14.0	DYmax [mm]	31.0	24.0
2	IpMYmax [kNm]	0.30	0.30	IpMYmax [kNm]	0.39	0.40
3	spMYmax [kNm]	0.01	0.01	spMYmax [kNm]	0.01	0.01

No.	Earthquake level-1: Petrovac PGA = 0,71 g			Earthquake level-2: Petrovac PGA = 1,7 g		
	Notation	Max (+)	Max (-)	Notation	MaxD (+)	MaxD (-)
1	DYmax [mm]	15.0	12.0	DYmax [mm]	31.0	34.0
2	IpMYmax [kNm]	0.29	0.31	IpMYmax [kNm]	0.41	0.47
3	spMYmax [kNm]	0.00	0.00	spMYmax [kNm]	0.01	0.01

bearings only over the central piers in model M2, without SF-ED-4C-L1R-T1 devices was (in this case only) conditioned by the intention to reduce the transfer of large seismic forces at the top of the central piers, and to ensure reduction of bearing moments at the fixation points of central piers. However, the use of other options is not restricted. Figure 22 comparatively shows the response time histories of My bearing moment at the bottom of longer piers under strong and very strong intensity of the El Centro earthquake. The peak values of the moments are very small and amount to IpMymax = 0.30 kN and IpMymax = 0.40 kN, respectively.

Figure 23 comparatively presents the response time histories of moment My of the shorter piers obtained under the strong and very strong El Centro earthquake. The obtained values of maximum moments are even smaller, amounting to spMymax = 0.011 kN and spMymax = 0.015 kN, respectively. Finally, Table 8 shows the most important parameters of the responses under both earthquakes and their two intensities. More precisely, it shows the positive and negative peak values of displacements in γ -direction and the moment components for central piers My. Peak displacements obtained for model M2 are of the same order as displacements obtained for the case of the previously analysed model M1. This is logical because two identical SF-ED devices existed in both cases, and because the influence of different number of seismic isolators is not significant due to their very low horizontal stiffness. The following most important conclusions can be made based on the analysis of seismic response of the composed new three-span USI-SF bridge system subjected to seismic excitation of strong and very strong intensity:

- seismic energy dissipation performances of the new SF-ED types of devices can very successfully be designed and harmonized with real-life needs;
- under numerous iterative dynamic cycles of positive and negative displacements, the new SF-ED devices show high reliability, adaptability and stability of the main parameters that control their hysteretic behaviour;
- the installation of SF-ED devices can be regarded as a considerable contribution to the improvement of seismic performance of isolated bridges subjected to strongest earthquakes;

- considering specific structural geometry, the new SF-ED devices ensure conditions for adopting mechanical properties required for their wider application;
- it is demonstrated with this study that the application of SF-ED devices is a reliable and advanced engineering concept, actually representing very efficient option for seismic protection of isolated bridges subjected to strong and very strong earthquake action.

8. Modelling and earthquake response characteristics of assembled classical three-span bridge prototype model M3

The seismic behaviour of the comparative three-span bridge prototype model assembled by implementation of a common classical bridge structural system considered here as Model 3 was analysed taking into account the outcome of previous studies and in order to provide comparative results that will demonstrate the above stated potential advantages of the USI-SF system. The assembled three-span bridge prototype model M3 represents a characteristic classical structural option. The existence of movable bearings was simulated on the left-side and right-side abutments. In this case, the movable bearings on the two abutments of the superstructure were created from the same previously investigated DSRSB devices, two at the left and two at the right end indicated by 1, 2 and 3, 4.

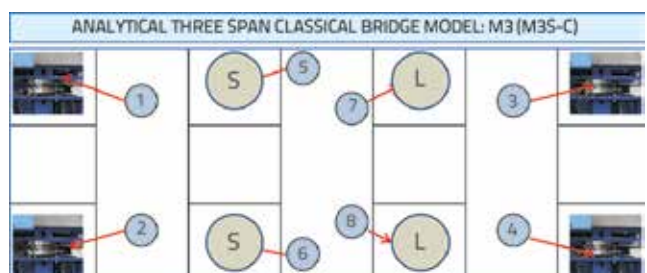


Figure 24. Positions of DSRSB devices and hinged connections on short and long piers of the assembled classical three-span large-scale bridge prototype model M3

Figure 24. A hinged connection 5 and 6 was modelled over two shorter central piers indicated by S, while hinged connections 7

and 8 were also considered over longer central piers indicated by L. Using the experimentally verified analytical model, the dynamic behaviour of the formulated classical three-span bridge prototype model M3 was analysed for the effect of strong and very strong earthquakes, which represented again some kind of an "analytical experiment". Also, in this case, central piers were treated as linear elements in the analytical model. The peak acceleration of the El Centro earthquake was analogously scaled to PGA = 0.77 g and PGA = 1.70 g, respectively, while the Petrovac earthquake was respectively scaled to PGA = 0.71 g and PGA = 1.70 g. The most characteristic results from all the performed analyses are selected and presented in Figure 25, Figure 26, Figure 27 and Table 9.

Figure 25 comparatively shows the time histories of superstructure displacements in y-direction (DY) under the

effect of the El Centro earthquake. In case of strong earthquake scaled to PGA = 0.77 g, the maximum displacement in y-direction amounts to maxDy = 22.0 mm, while for a strong earthquake scaled to PGA = 1.70 g the maximum displacement amounts to maxDy = 58.0 mm, Table 9. A similar tendency can also be observed in this table for the Petrovac earthquake. In this earthquake scaled to PGA = 0.71 g, maxDy = 49.0 mm was obtained, while under the same earthquake scaled to very strong intensity of PGA = 1.70 g, the maximum displacement amounted to maxDy = 115.0 mm. Also, in this case, due to simulation of direction of earthquake action at 45° with respect to the longitudinal axis of the bridge, the displacement components DX and DY were identical, while their values in earthquake direction are larger and are computed by multiplying the components by the factor of $f = \sqrt{2}$.

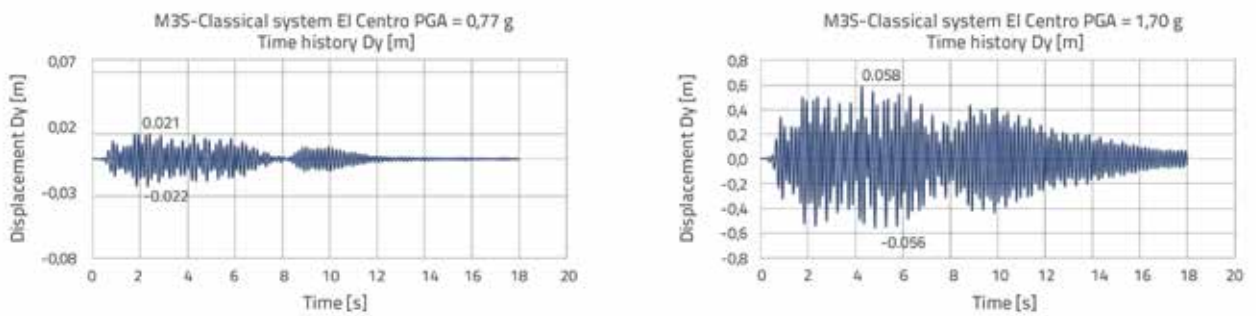


Figure 25. Classical bridge model M3: Displacement response in y-direction DY under El Centro earthquake scaled to PGA = 0.77 g and PGA = 1.70 g in shaking table direction

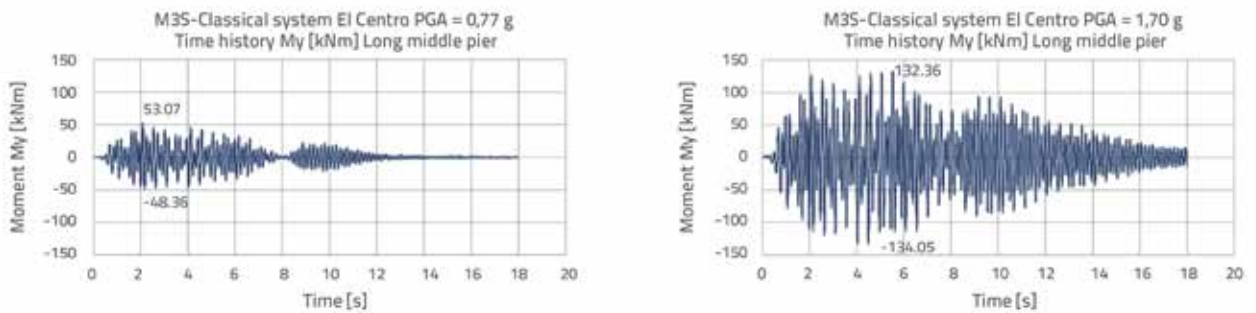


Figure 26. Classical bridge model M3: Moment response MY at fixed bottom point of long central pier under El Centro earthquake scaled to PGA = 0.77 g and PGA = 1.70 g in shaking table direction

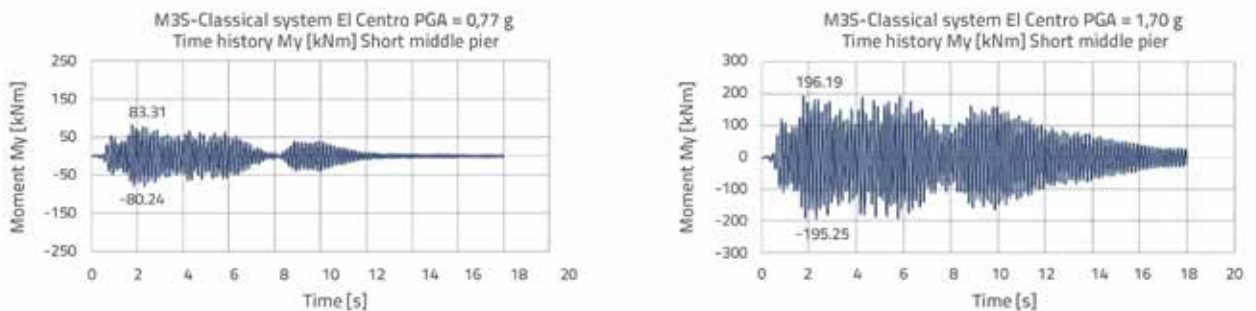


Figure 27. Classical bridge model M3: Moment response MY at fixed bottom point of short central pier under El Centro earthquake scaled to PGA = 0.77 g and PGA = 1.70 g in shaking table direction

Table 9. Computed γ -components of positive and negative values of selected characteristic parameters of USI-SF bridge model M3 for two intensity levels of El Centro and Petrovac earthquake

No.	Earthquake level-1: El Centro PGA = 0,77 g			Earthquake level-2: El Centro PGA = 1,7 g		
	Notation	Max (+)	Max (-)	Notation	Max (+)	Max (-)
1	DYmax [mm]	21.0	22.0	DYmax [mm]	58.0	56.0
2	IpMYmax [kNm]	53.1	48.4	IpMYmax [kNm]	132.4	134.0
3	spMYmax [kNm]	83.3	80.2	spMYmax [kNm]	196.2	195.2
No.	Earthquake level-1: Petrovac PGA = 0,71 g			Earthquake level-2: Petrovac PGA = 1,7 g		
	Notation	Max (+)	Max (-)	Notation	MaxD (+)	MaxD (-)
1	DYmax [mm]	45.0	49.0	DYmax [mm]	106.0	115.0
2	IpMYmax [kNm]	112.1	102.5	IpMYmax [kNm]	256.9	227.0
3	spMYmax [kNm]	173.8	184.4	spMYmax [kNm]	399.5	421.1

In this case, because the central piers had a hinged connection with the superstructure, the values of the bending moments at their bottom fixation point were far greater and very critical for such high levels of earthquake intensity. Figure 26 provides a comparative presentation of the time history responses of moments MY of longer piers under strong and very strong intensity of the El Centro earthquake. The peak values of the moments were very high and amounted to IpMymax = 53.1 kNm and IpMymax = 134.0 kNm, respectively.

Figure 27 comparatively shows the time history responses to moment MY of shorter piers obtained under the effect of the same strong and very strong El Centro earthquake. The obtained values of maximum bending moments were even greater, amounting to spMymax = 83.3 kNm and spMymax = 196.2 kNm, respectively. Analogously, Table 9 shows representative response parameters for both earthquakes and their two intensities. Specifically, the positive and negative peak displacement components of superstructure in γ -direction, and obtained moments MY for the central piers, are given. Based on the results from the performed analyses of seismic response of the assembled classical bridge system under the effect of earthquakes with strong and very strong intensities, the following known facts are exposed:

- The classical bridge system, which does not possess additional devices for seismic energy dissipation, is commonly exposed to large seismic forces attracting large moments to the supports of central piers with an open possibility for generation of deep nonlinearity, severe damage or complete failure;
- Under strong and very strong earthquake, the capacity for deformation of the critical cross-sections can be considerably exceeded at plastic hinges;
- Seismic safety of the classical systems of highway bridge structures is commonly assured by application of actual seismic design codes and classical design methods.

However, if classically designed structures are exposed to very strong earthquakes, unacceptable serious damage or complete failure occur very frequently. Nevertheless, the proposed USI-

SF system can be practically used for efficient and rapid seismic upgrading of a large number of existing highway bridges with inadequate seismic safety.

9. Conclusions

Based on research results from extensive experimentally validated theoretical studies focusing on the development of an advanced method for seismic upgrading of isolated bridges with new SF-ED devices, the following conclusions can be made:

- Seismic protection level of isolated bridges with optimized new DSRSB devices, and seismically upgraded by installation of newly designed SF-ED devices, may be very significantly increased ensuring a greater seismic safety of bridge structures under strong and very strong earthquakes;
- The presented comprehensive study results on seismic performance of the analysed single-span and three-span innovative USI-SF bridge prototype models under simulated real earthquake effects scaled to high and very high intensity represented by PGA = 0.70 g (0.71 g to 0.77 g) and PGA = 1.70 g have shown very high capability of the new USI-SF system for qualitative improvement of seismic protection of multi-span highway bridges with optimum distribution of seismic isolation SI and energy dissipation SF-ED devices;
- The new USI-SF seismic protection system enabled a very significant reduction of peak displacement of bridge superstructure under a largely increased earthquake intensity. Specifically, considering the presented results for PGA increase from PGA = 0.70 g to PGA = 1.70 g, representing an increase of about 240 %, a significantly lower displacement increase of about 95 % and 85 % was obtained in the case of the studied single-span and three-span USI-SF bridge prototype systems;
- The obtained results from comparatively studied classically designed three-span bridge prototype clearly show the existence of uncontrolled effect of large seismic forces and critical moments in central piers, often producing severe damages or total collapses;

- The developed three new types of versatile SF-ED devices represented with specific geometrical parameter $L = 1R$, $L = 2R$ and $L = 3R$ show excellent hysteretic behaviour characteristics under repeated cyclic loads. The proposed full and partial assembling variants exhibit highly favourable possibilities for their typified design and production according to actual application needs;
- The developed experimentally verified technology for seismic upgrading of isolated bridges, involving installation of the innovative SF-ED devices, is a very efficient engineering tool for reliable seismic protection of highway bridges exposed to strong and very strong future earthquakes.

REFERENCES

- [1] Kelly, J.M.: A seismic base isolation: A review and bibliography, *Soil Dynamics and Earthquake Engineering*, 5 (1986), pp. 202-216, [https://doi.org/10.1016/0267-7261\(86\)90006-0](https://doi.org/10.1016/0267-7261(86)90006-0)
- [2] Kunde, M.C., Jangid, R.S.: Seismic behaviour of isolated bridges: A-state-of-the-art review, *EJSE, Electronic Journal of Structural Engineering*, 3 (2003).
- [3] Turkington, D.H., Carr, A.J., Cooke, N., Moss, P.J.: Seismic design of bridges on Lead-rubber bearings, *Journal of Structural Engineering, ASCE*, 115 (1989) a, pp. 3000-3016.
- [4] Robinson, W.H.: Lead-rubber hysteretic bearings suitable for protecting structures during earthquakes, *Earthquake Engineering and Structural Dynamics*, 10 (1982), pp. 593-604, <https://doi.org/10.1002/eqe.4290100408>
- [5] Dolce, M., Cardone, D., Palermo, G.: Seismic isolation of bridges using isolation systems based on flat sliding bearings. *Bull Earthq. Eng.* 14:1285-1310, 5 (2007), pp. 491-509.
- [6] Iemura, H., Taghikhany, T., Jain, S. K.: Optimum Design of Resilient Sliding Isolation System for Seismic Protection of Equipments. *Bull Earthq. Eng.*, 5 (2007), pp. 85-103, <https://doi.org/10.1007/s10518-006-9010-5>
- [7] Kartoum, A., Constantinou, M.C., Reinhorn, A.M.: Sliding isolation system for bridges: Analytical study, *Earthquake Spectra*, 8 (1992), pp. 345-372, <https://doi.org/10.1193/1.1585685>
- [8] Wang, Y.P., Chung, L., Wei, H.L.: Seismic response analysis of bridges isolated with friction pendulum bearings, *Earthquake Engineering and Structural Dynamics*, 27 (1998).
- [9] Zayas, V.A., Low, S.S., Mahin, S.A.: A simple pendulum technique for achieving seismic isolation, *Earthquake Spectra*, 6 (1990), pp. 317-334, <https://doi.org/10.1193/1.1585573>
- [10] Mokha, A., Constantinou, M.C., Reinhorn, A.M.: Teflon bearings in seismic base isolation I: Testing, *Journal of Structural Engineering, ASCE*, 116 (1990), pp. 438-454, [https://doi.org/10.1061/\(ASCE\)0733-9445\(1990\)116:2\(438\)](https://doi.org/10.1061/(ASCE)0733-9445(1990)116:2(438))
- [11] Constantinou, M.C., Kartoum, A., Reinhorn, A.M., Bradford, P.: Sliding isolation system for bridges: Experimental study", *Earthquake Spectra*, 8 (1992), pp. 321-344, <https://doi.org/10.1193/1.1585684>
- [12] Skinner, R.I., Kelly, J.M., Heine, A.J.: Hysteretic Dampers for earthquake resistant structures, *Earthquake Engineering and Structural Dynamics*, 3 (1975), pp. 287-296, <https://doi.org/10.1002/eqe.4290030307>
- [13] Guan Z., Li, J., Xu, Y.: Performance Test of Energy Dissipation Bearing and Its Application in Seismic Control of a Long-Span Bridge, *Journal of Bridge Engineering, ASCE*, 2010, [https://doi.org/10.1061/\(ASCE\)BE.1943-5592.0000099](https://doi.org/10.1061/(ASCE)BE.1943-5592.0000099)
- [14] Tsopelas, P., Constantinou, M.C., Kim, Y.S., Okamoto, S.: Experimental study of FPS system in bridge seismic isolation, *Earthquake Engineering and Structural Dynamics*, 25 (1996) a, pp. 65-78, [https://doi.org/10.1002/\(SICI\)1096-9845\(199601\)25:1<65::AID-EQE536>3.0.CO;2-A](https://doi.org/10.1002/(SICI)1096-9845(199601)25:1<65::AID-EQE536>3.0.CO;2-A)
- [15] Dolce, M., Filardi, B., Marnetto, R., Nigro, D.: Experimental tests and applications of advanced biaxial elastoplastic device for the passive control of structures, *Proc. of 4th World congress on joint sealants and bearing systems for concrete structures, Sacramento, California (USA)*, 1996.
- [16] Ene, D., Yamada, S., Jiao, Y., Kishiki, S., Konishi, Y.: Reliability of U-shaped steel dampers used in base-isolated structures subjected to biaxial excitation, *Earthquake Engineering & Structural Dynamics*, 46 (2017) 4, pp.621-639, <https://doi.org/10.1002/eqe.2806>
- [17] Oh, S.H., Song, S.H., Lee, S.H. et al.: Seismic response of base isolating systems with U-shaped hysteretic dampers, *Int. Journal of Steel Structures*, 12 (2012) 2, pp 285-298, <https://doi.org/10.1007/s13296-012-2011-0>
- [18] Jankowski, R., Wilde, K., Fujino, Y.: Pounding of superstructure segments in isolated elevated bridge during earthquakes, *Earthquake Eng. and Struct. Dynamics*, 27 (1998), pp. 487-502, [https://doi.org/10.1002/\(SICI\)1096-9845\(199805\)27:5<487::AID-EQE738>3.0.CO;2-M](https://doi.org/10.1002/(SICI)1096-9845(199805)27:5<487::AID-EQE738>3.0.CO;2-M)
- [19] Tubaldi, E., Mitoulis, S. A., Ahmadi, H., Muhr, A.: A parametric study on the axial behaviour of elastomeric isolators in multi-span bridges subjected to horizontal seismic excitations. *Bull Earthq. Eng.*, 14 (2016), pp. 1285-1310, <https://doi.org/10.1007/s10518-016-9876-9>
- [20] Serino, G., Occhiuzzi, A.: A semi-active oleodynamic damper for earthquake control: Part 1: Design, manufacturing and experimental analysis of the device. *Bull Earthq. Eng.*, 1 (2003), pp. 269-301, <https://doi.org/10.1023/A:1026340911767>
- [21] Mayes, R.L., Buckle, I.G., Kelly, T.E., Jones, L.R.: AASHTO Seismic isolation design requirements for highway bridges, *Journal of Structural Engineering, ASCE*, 118 (1992), pp. 284-304, [https://doi.org/10.1061/\(ASCE\)0733-9445\(1992\)118:1\(284\)](https://doi.org/10.1061/(ASCE)0733-9445(1992)118:1(284))

Acknowledgements

Extensive experimental and analytical research has been realized at IZiIS, University "SS Cyril & Methodius", Skopje, in the framework of the three year innovative NATO Science For Peace and Security Project: *Seismic Upgrading of Bridges in South-East Europe by Innovative Technologies (SFP: 983828)*, with participation of five countries: Macedonia: D. Ristic, Leader & PPD-Director, Germany: U. Dorka, NPD-Director, Albania: A. Lako, Bosnia & Herzegovina: D. Zenunovic & Serbia: R. Folic. Creation of RESIN Laboratory, as a new open testing lab of Regional Seismic Innovation Network involving young scientists, was an accepted long-term specific task. The extended NATO support for realization of the integral long-term and costly innovative research project is highly appreciated.

- [22] Unjoh, S., Ohsumi, M.: Earthquake response characteristics of super-multispan continuous menshin (seismic isolation) bridges and the seismic design, ISET Journal of Earthquake Engineering Technology, 35 (1998), pp. 95-104.
- [23] Ristic, J., Misini, M., Ristic, D., Guri, Z., Pllana, N.: Seismic upgrading of isolated bridges with SF-ED devices: Shaking table tests of large-scale model, GRAĐEVINAR, 70 (2017) 6, pp. 463-485, <https://doi.org/10.14256/JCE.2147.2017>
- [24] ANSYS Mechanical: Finite element analysis (FEA) software, ANSYS, Inc., USA.
- [25] Candeias, P., Costa, A.C., Coelho, E.: Shaking table tests of 1:3 reduced scale models of four story unreinforced masonry buildings, 13th World Conf. on Earthquake Eng., Vancouver, Paper: 2199, 2004.
- [26] Ristic, D., Ristik, J.: New Integrated 2G3 Response Modification Method for Seismic Upgrading of New and Existing Bridges, 15th World Conference on Earthquake Engineering, (WCEE), Lisbon, Portugal, 2012.
- [27] Ristic, D.: Nonlinear Behaviour and Stress-Strain Based Modelling of Reinforced Concrete Structures Under Earthquake Induced Bending and Varying Axial Loads, Doctoral Dissertation, School of Civil Engineering, Kyoto University, Kyoto, Japan, 1988.
- [28] Ristik, J.: Comparative Seismic Analysis of RC Bridge Structure Applying Macedonian Seismic Design Regulations and Eurocodes, MSc Thesis, Department for Theory of Structures, University SS Cyril and Methodius, Skopje, Macedonia, 2011.
- [29] Ristik, J.: Modern Technology for Seismic Protection of Bridge Structures Applying New System for Modification of Earthquake Response, PhD Thesis, Institute of Earthquake Engineering and Engineering Seismology (IZIIS), University SS Cyril and Methodius, Skopje, Macedonia, 2016.
- [30] Wilson, E.L.: Three-Dimensional Static and Dynamic Analysis of Structures: A Physical Approach With Emphasis on Earthquake Engineering, Berkeley, California: Third Ed., 2002.
- [31] Wilson, E.L., Habibullah, A.: SAP2000, Structural and earthquake engineering software, Computers and Structures Inc., Berkeley, California, USA.